



A sensitive and selective procedure for the voltammetric determination of brilliant indigo and acid yellow 23 at surfactant modified graphene paste electrode

C. Raril and J. G. Manjunatha*

*Department of Chemistry, FMKMC College, Mangalore University Constituent College, Karnataka, India

Received 22 May 2019,
Revised 23 June 2019,
Accepted 24 June 2019

Keywords

- ✓ Brilliant indigo,
- ✓ Acid yellow 23,
- ✓ Voltammetric determination,
- ✓ Differential pulse voltammetry,
- ✓ cyclic voltammetry,

manju1853@gmail.com

Phone: ++91- 08272228334.

Abstract

The voltammetric response of brilliant indigo and acid yellow 23 on the surface of graphene paste electrode modified with nonionic surfactant was studied in the buffer media at different pH by cyclic voltammetry and differential pulse voltammetry Vs. saturated calomel electrode. Cyclic voltammograms were recorded in the potential range from 0 V to 0.8 V for brilliant indigo, and 0.60 to 1.2 V for acid yellow 23 shows reversible and irreversible response respectively. The developed electrochemical sensor shows good electrocatalytic activity to the oxidation of brilliant indigo and acid yellow 23 by giving elevated peak current than those obtained for the bare electrode. At the optimized conditions, the anodic peak current of brilliant indigo and acid yellow 23 proportional to the concentration ranges from 3.5×10^{-6} - 1.5×10^{-5} M and 1×10^{-5} - 6×10^{-5} M with the limit of detection of 0.24 μ M and 0.25 μ M. The proposed method offers rapid, simple, selective, and cost-effective analysis. Also, this developed electrode exhibited good selectivity, stability, repeatability, and has been successfully used to determine the real sample with a satisfactory result.

1. Introduction

Food additives generally improve the appearance, flavor, taste, color, and preservation. Past few decades, synthetic colorants have been extensively used in the food industry [1-2]. Brilliant indigo (BI) or indigo blue and acid yellow 23 (AY 23) both are synthetic azo dye with aromatic ring structure were harmful to human health [3-4]. Generally, azodyes are electrochemically active both in oxidation and reduction region. Nowadays, many methods were used in the treatment of dye effluents, such as physical [5], chemical [6], physio-chemical [7], and biological [8]. These techniques were relatively expensive, ineffective, or can cause secondary pollution. So Reliable analytical methods are required for the simultaneous analysis of BI and AY 23. Electrochemical technology has attracted growing interest as an alternative to conventional methods [9-14]. Cyclic voltammetry provides an extreme insight into the redox reactions of biologically active molecules and can be used to study the redox potential, rate of heterogeneous electron transfer kinetics and to detect chemical reaction that follows electron transfer.

Graphene, a waved plane of Sp^2 - bonded monolayer carbon atoms excellently arranged in a honeycomb lattice, and used as an electrode material because due to its excellent structural, physical, and chemical properties. There is much literature, where the graphene electrode was used to study some biological molecules, including DNA [15], hydrogen peroxide [16], acetaminophen, ascorbic acid [17,18], uric acid and flufenamic acid [19-21], etc. Surfactants have extensively used in chemistry, especially in electrochemical processes to change the electrical properties of the electrode solution interface and electrochemical process through adsorption.

We report herein the electrochemical oxidation properties of brilliant indigo and acid yellow 23 at nonionic surfactant modified graphene paste electrode by cyclic voltammetry. The performance of the fabricated electrode for the analysis of brilliant indigo and acid yellow 23 with respect to sensitivity and the linear range was assessed. The application of the developed electrode in the real sample also processes. The oxidation mechanism of brilliant indigo (Figure 1a) and acid yellow 23 (Figure 1b) were studied.

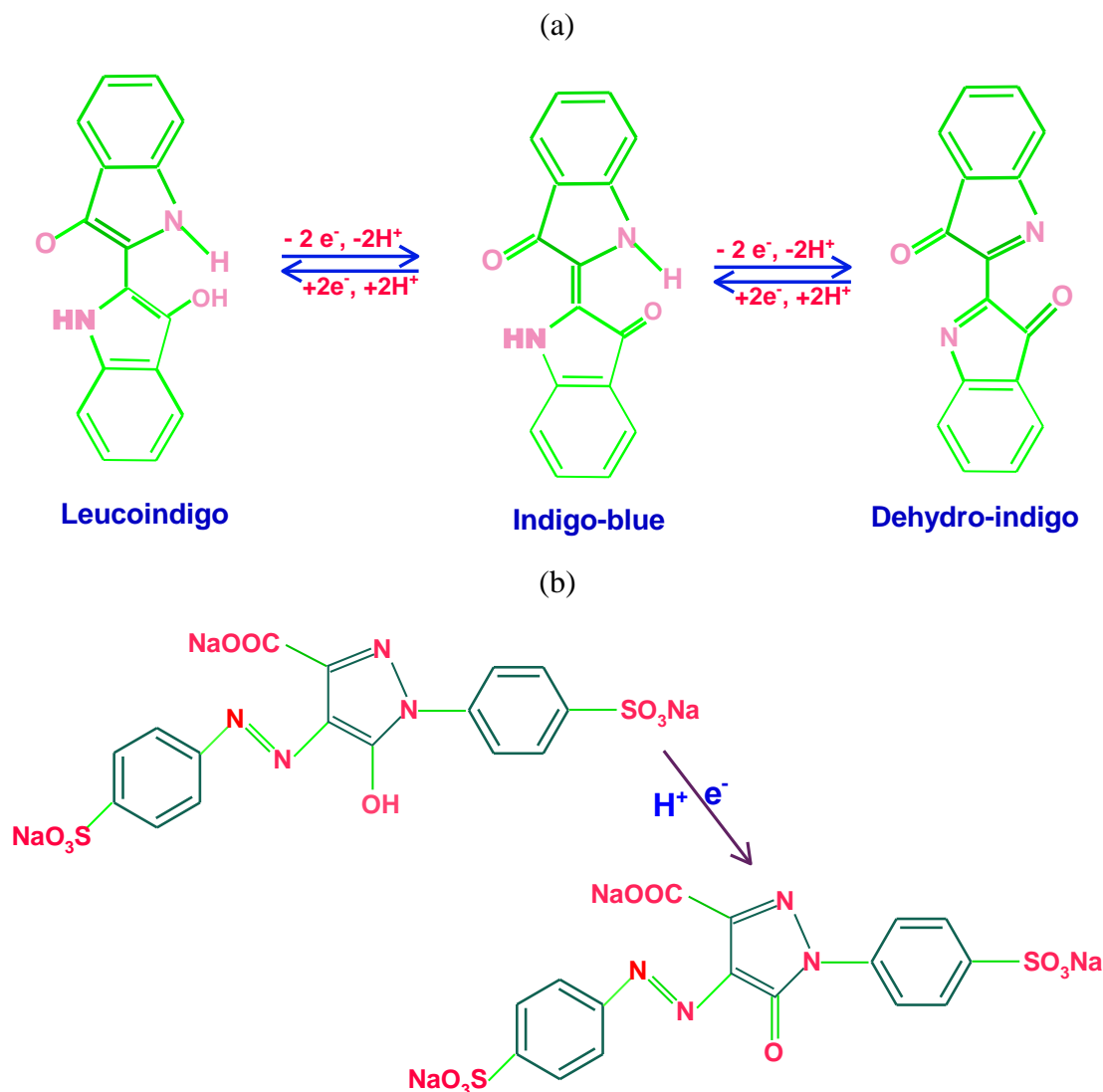


Figure 1. Oxidation mechanism of BI (a) and AY 23 (b)

2. Materials and methods

2.1. Materials and Chemicals

Graphene was obtained from TCI, Silicone oil and, Acid yellow 23 was purchased from nice chemical, India, BI received from Molychem, India Pvt. Ltd. A stock solution (BI- 25×10^{-5} M, Acid Yellow 23 - 25×10^{-4} M) was prepared in distilled water. TX-100, disodium hydrogen phosphate and monosodium hydrogen phosphate were obtained from himedia. The phosphate buffer solution was prepared by mixing an appropriate amount of 0.1 M disodium hydrogen phosphate and monosodium hydrogen phosphate

2.2. Instrumentation

All the experiments were carried out with an electrochemical analyzer CHI6038E (USA) connected to an electrochemical cell, which is equipped the conventional three-electrode system with a BGPE and TX-100MGPE as a working electrode, a saturated calomel electrode (SCE) and a platinum wire as reference electrode and auxiliary electrode. Field emission scanning electron microscopy (FESEM) obtained from DST-PURSE Laboratory, Mangalore University, Oxford instrument.

2.3. Development of Electrochemical sensor electrodes

The graphene paste electrode was prepared by mixing thoroughly graphene and a binder (silicone oil) at composition 60:40 (w/w %) using an agate mortar and pestle and was allowed to homogeneous for 20 minutes. A portion of paste was packed into a teflon tube having 3 mm diameter. Electrode surface was smoothed with tissue paper to produce a reproducible surface. TX-100MGPE was prepared by the immobilization technique and which was used for further experiments.

3. Results and Discussions

3.1. Characterization of Developed Electrode

Figure 2 showed the morphologies of bare (Figure 2a) and modified electrode (Figure 2b) characterized by FESEM. Compared with the bare electrode, modified electrode shows the agglomerates of surfactant uniformly covered on the bare surface, because surfactant molecules were immobilized on to the bare surface, indicating that the bare electrode was successfully modified with surfactant.

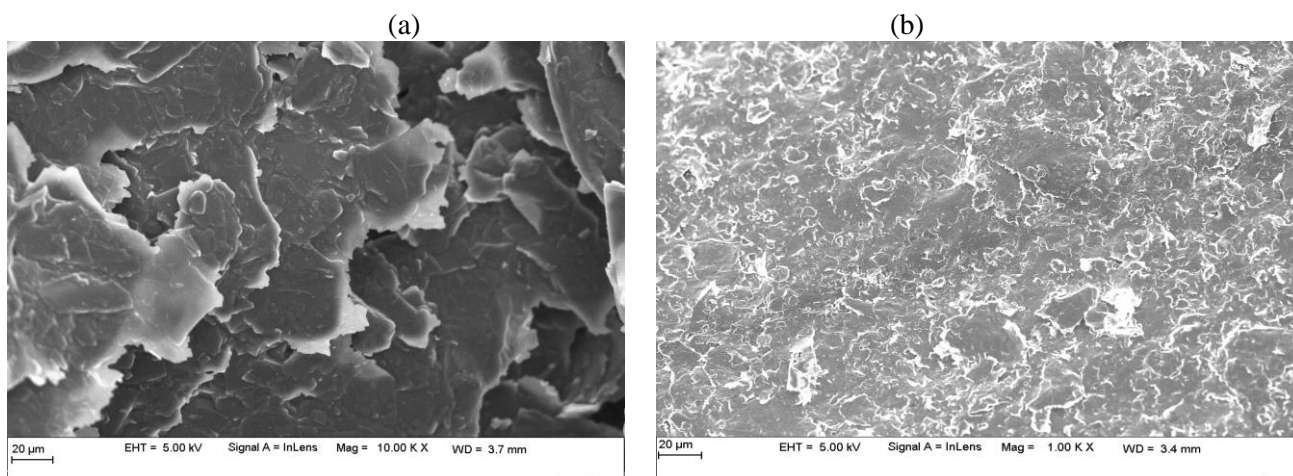


Figure 2. FESEM image of bare (a) and TX-100MGPE (b)

3.2. Optimization of surfactant concentration

The amount of SDS concentration on the surface of the bare electrode was optimized. As seen in figure 3, the maximum peak current this was observed when the surfactant concentration was 10 μL . A further increase in the concentration of surfactant led to a decrease of the peak current. This was explained by critical micelle concentration (CMC) which reached at 10 μL . Hence, 10 μL was chosen for the optimum volume for the sensing properties of BI. Figure 3b, shows the relation between the concentration variation of surfactant and the peak current.

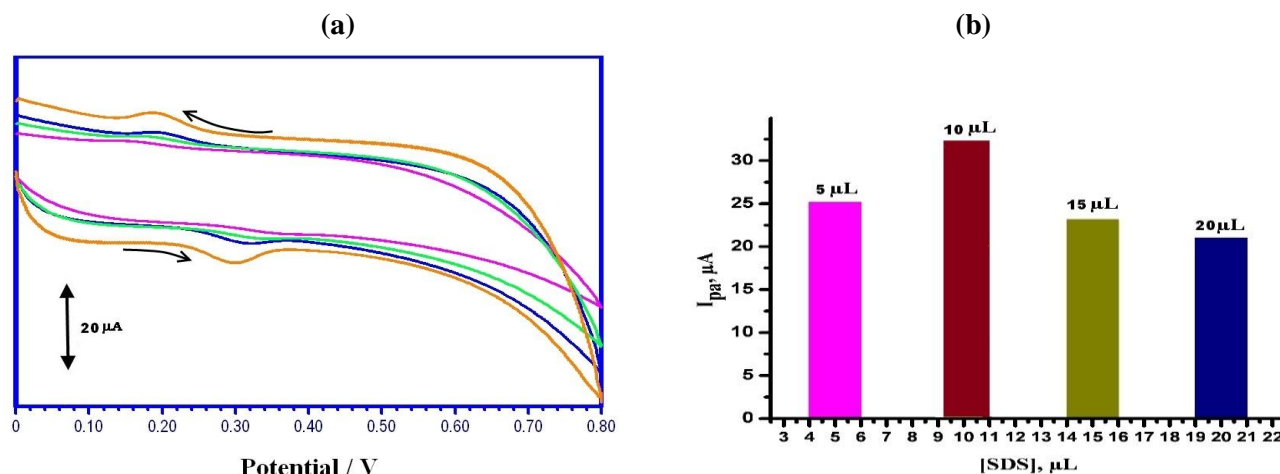


Figure 3. (a) Cyclic voltammogram of 1×10^{-5} M BI on a graphene paste electrode at different concentration of SDS in 0.1 M PBS (7.5 pH) at the scan rate of 0.1 V/s, (b) I_{pa} Vs [SDS]

3.3. Electrochemical Measurements

The electrochemical measurement of the developed electrode was conducted using the $\text{K}_2\text{Fe}(\text{CN})_6$. Figure 4, shows the electrochemical behavior of $\text{K}_2\text{Fe}(\text{CN})_6$ in 0.1 M KCl at bare (curve a) and modified electrode (curve b) in the potential window -0.2 V to 0.6 V at the sweep rate of 0.1 V/s. A well-defined reduction peak was perceived at a modified electrode contrast to the bare electrode. According to figure 4, curve a, the oxidation peak of $\text{K}_2\text{Fe}(\text{CN})_6$ is located at 0.212 V with an anodic current response of 11.81 μA . Modified electrode shows the oxidation peak at 0.198 V with the oxidation peak current of 50.09 μA . The ratio of peak currents for the modified electrode was 1.12, which explains the electrode process was quasi-reversible. The current response is related to the square root of the scan rate with the following equation:

$$I_p = Kn^{3/2} AD^{1/2} C^b \nu^{1/2} \quad [22]$$

Where the constant $K=2.69 \times 10^5$; n is the number of moles of electrons transferred (1) per mole of electroactive species; A is the area of the electrode in cm^2 ; D is the diffusion coefficient ($6.70 \times 10^{-6} \text{ cm}^2/\text{s}$); C^b is the concentration in mol/L (1 mM); and ν is the scan rate in V/s. The surface area of the developed electrodes was calculated and obtained as 0.0175 cm^2 (bare), 0.07 cm^2 (modified). The high effective surface area would positively contribute to the improvement of the current response and conductivity shows that the good electrochemical behavior of $\text{K}_2\text{Fe}(\text{CN})_6$ at the modified electrode.

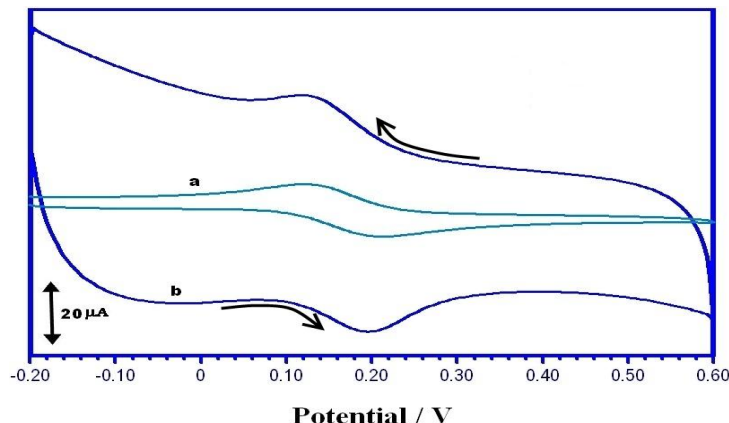


Figure 4. Cyclic voltammogram of 1 mM $\text{K}_2\text{Fe}(\text{CN})_6$ / 0.1M KCl at BGPE (a) & TX-100MGPE (b) at the scan rate of 0.1 V/s

3.4. Cyclic voltammetric responses of BI and AY 23

Cyclic voltammetric response of BI ($1 \times 10^{-5} \text{ M}$) at modified and bare electrode was investigated in 0.1 M PBS (pH 7.5) at the sweep rate of 0.1 V/s. For bare carbon paste electrode the anodic peak current observed at 0.266 V with the current response of $2.4 \mu\text{A}$ but the electrochemical reaction kinetics was improved at modified electrode, where anodic peak appears at 0.289 V with a current response of $32.5 \mu\text{A}$, which is larger to the current was observed for bare electrode, this was explained as the larger surface area of the modified electrode improve the electrode kinetics. Figure 5a shows the cyclic voltammogram of and blank solution (curve a), bare (curve b) and modified (curve c).

Figure 5b shows the voltammetric behavior of AY 23 ($1 \times 10^{-4} \text{ M}$) at the bare and modified electrode in 0.1 M PBS (pH 7.5) at the scan rate of 0.1 V/s. The current response obtained at the modified electrode is double to that of the modified electrode and shows only anodic peak with no cathodic peak in the reverse scan, indicating the irreversible property of the electrode reaction.

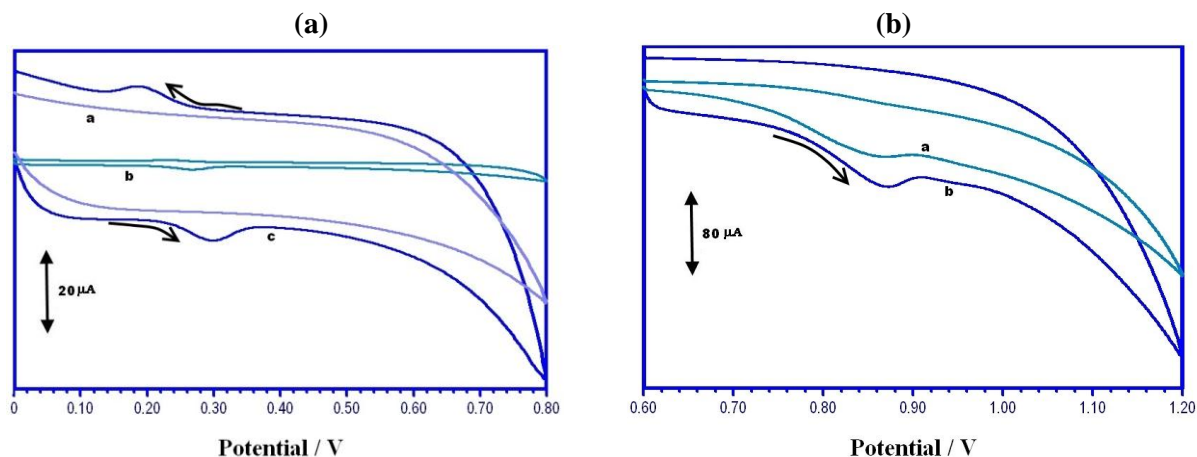


Figure 5. (a) Cyclic voltammogram of BI ($1 \times 10^{-5} \text{ M}$) at BGPE (curve b), TX-100MGPE (curve c) for blank solution (curve a) in 0.1 M PBS (pH 7.5) at the scan rate of 0.1 V/s, (b) Cyclic voltammogram of AY 23 ($1 \times 10^{-4} \text{ M}$) at BGPE (curve a) and at TX-100MGPE (curve b)

3.5. Influence of pH

The pH of the solution has a significant effect on the electrochemical response of the electroactive on the electrode surface; therefore, pH optimization of the solution seems to be imperative to obtain the electrocatalytic oxidation of BI. Figure 6a shows the cyclic voltammogram of BI at different pH ranges from 6.0-8.0 at the scan

rate of 0.1 V/s. It is noticed that the current response maximum was obtained buffer having pH 7.5 (Figure 6b). Thus, pH 7.5 was employed for further studies. It was noticed that the peak potential was shifted towards less positive when the pH increased from 6.0 to 8.0. The pH dependency of the oxidation peak potential indicates that protonation is taking part in the charge transfer process. The plot of E_{pa} Vs pH was found to be linear. This linear relationship can be described by the following equation E_{pa} (V) = 0.9246-0.0814 pH (Figure 6c) with the correlation coefficient of 0.99.

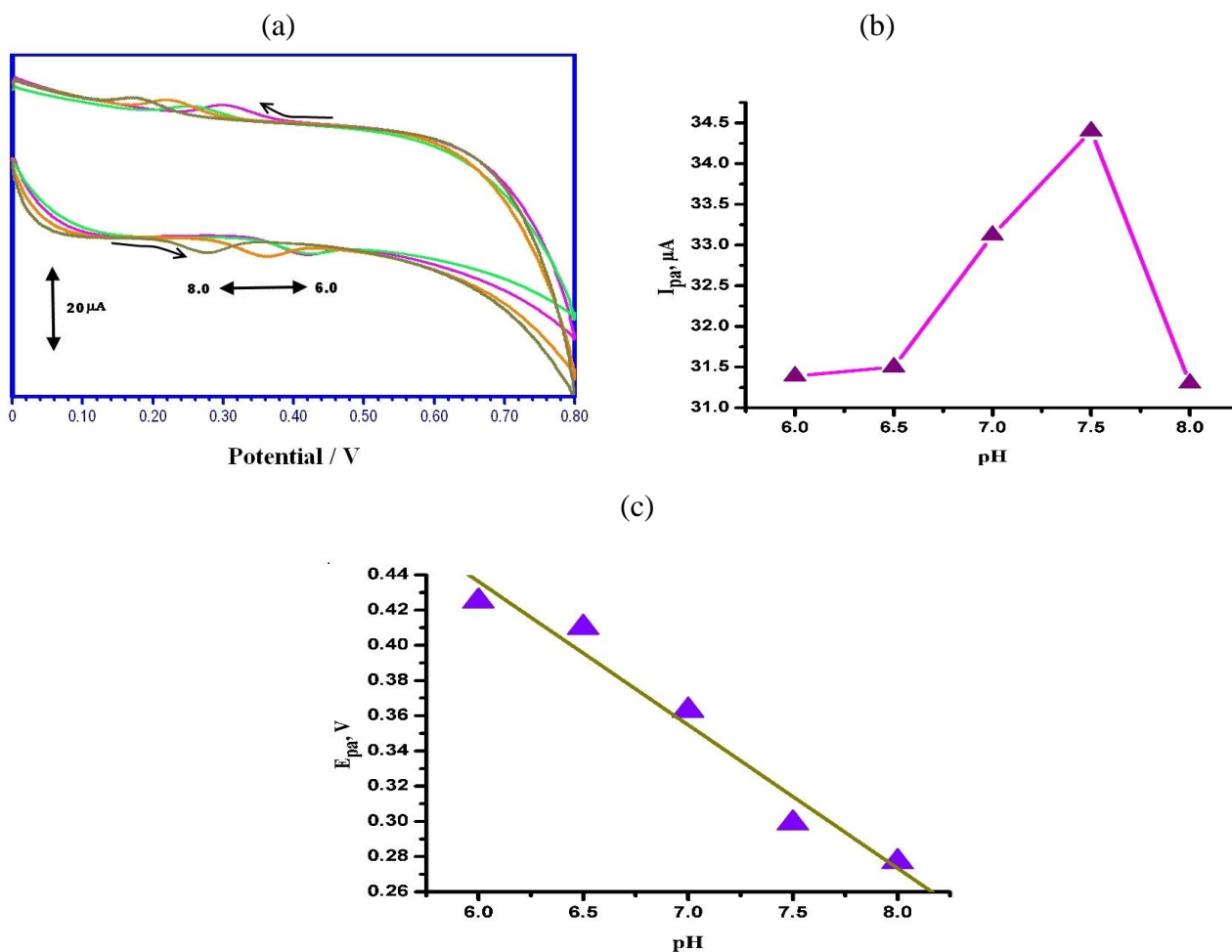


Figure 6. (a) Cyclic voltammogram of BI (1×10^{-5} M) at TX-100MGPE in 0.1 M PBS at different pH values 6.0,6.5,7.0,7.5,8.0, (b) I_{pa} Vs pH (c) E_{pa} Vs pH

3.6. Effect of Sweep rate

The influence of the scan rate on the peak current and peak potential under 1×10^{-5} M BI was discussed in order to study the reaction mechanism. The effect of sweep rate on the peak current and peak potential of BI at TX-100MGPE was studied by varying the scan rate from 0.1 to 0.3 V/s. Figure 7a shows that the CVs of 1×10^{-5} M BI at the scan rate ranging from 0.1 to 0.3 V/s. Peak current of BI increased with the scan rate. Peak current of BI showed a linear dependence on the scan rate as shown in the Figure.7b with the linear regression equation of I_{pa} (μA) = 8.75 + 247.09 v (V/s) with the correlation coefficient of 0.998. These results indicate that the electrode process is adsorption controlled [23, 24]. The charge transfer coefficient α , and electron transfer rate constant was calculated by the following equations:

$$E_{pa} = E^0 + \frac{RT}{(1-\alpha)nF} \ln v$$

$$\log K_s = \alpha \log(1-\alpha) + (1-\alpha) \log \alpha - \log \frac{RT}{nFv} - (1-\alpha) \frac{\alpha F \Delta E_p}{2.3RT} \quad [25, 26]$$

Where α is the charge transfer coefficient, n is the number of electrons transferred, K_s is the electron transfer rate constant, E^0 is the formal potential, F is the Faraday constant, E_{pa} is the anodic peak potential. It was seen that the charge transfer coefficient and electron transfer rate constant are in the value of 0.76 and $1.1S^{-1}$

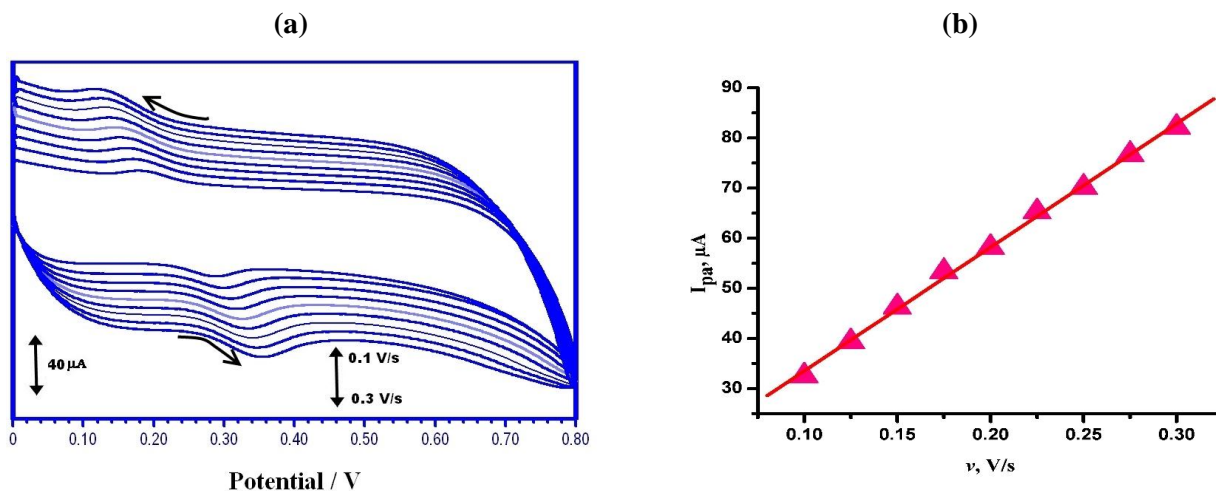


Figure 7. (a) Cyclic voltammogram of BI (1×10^{-5} M) at TX-100MGPE at different scan rates (0.1 to 0.3 V/s) in 0.1 M PBS (7.5 pH) (b) I_{pa} Vs v

The cyclic voltammogram at various scan rates was performed at modified graphene paste electrode contains 1×10^{-4} M AY 23 (Figure 8a). With the rise of scan rate peak current also increased with the linear regression equation of I_{pa} (μA) = $45.22 + 748.3 v$ (V/s) (Figure 8b) with the correlation coefficient of 0.99, shows that the electrode process was adsorption controlled [27].

For irreversible electrode process, E_{pa} was given by the following equation,

$$E_p(V) = E^o + \frac{RT}{\alpha nF} \ln \frac{RTK_s}{\alpha nF} + \frac{RT}{\alpha nF} \ln v \quad [28]$$

Where, E^0 is the formal standard potential, R, T, F were constant, K_s is the heterogeneous reaction rate constant, α is the charge transfer coefficient. From the graph E_{pa} Vs $\ln v$ (not shown), the slope is equal to $RT/\alpha nF$. For an irreversible electrode process, α value is usually assumed as 0.5. The electron transfer in the reaction was obtained to be $0.933 \sim 1$ and was theoretically close to 1.

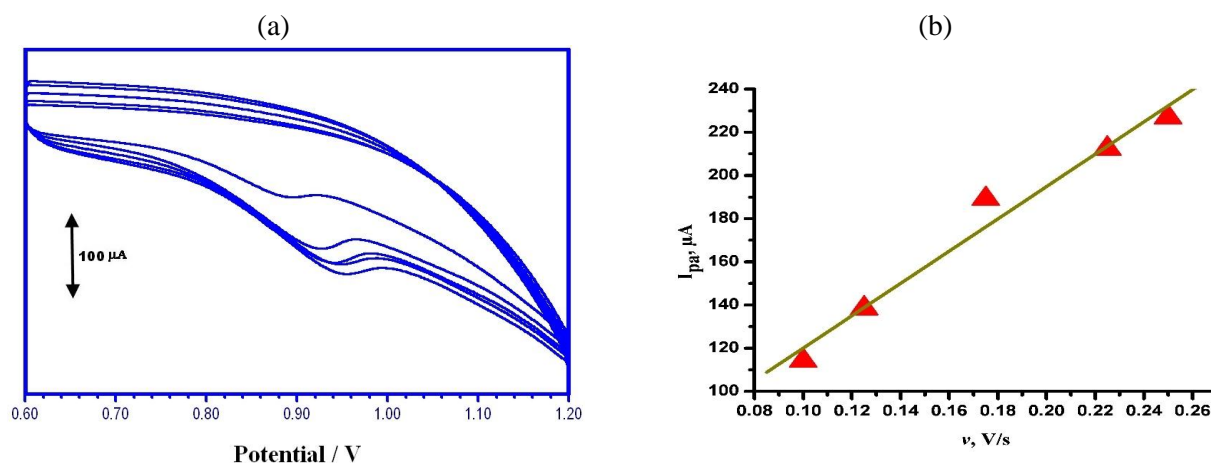


Figure 8. (a) Cyclic voltammogram of AY 23 (1×10^{-4} M) at TX-100MGPE at different scan rates in 0.1 M PBS (7.5 pH) (b) I_{pa} Vs v

3.7. Calibration Curve and Detection limit

Peak current of BI and AY 23 oxidation at the surface of the modified electrode can be used for the resolution of BI and AY 23 in the solution. Therefore CV technique was used to find out the relation between peak current and the concentration. Under the optimized condition, the different concentration of BI and the relation with the peak current are shown in figure 9a. The current response was linearly varied with the concentration of BI in the range 3.5×10^{-6} to 1.5×10^{-5} M. The linear regression equation was I_{pa} (A) = $1.9 \times 10^{-5} + 0.45 C$ (M) with the coefficient correlation of 0.99. Figure 9b shows the relation between concentration and peak current of AY 23 in 0.1 M PBS at 7.5 pH.

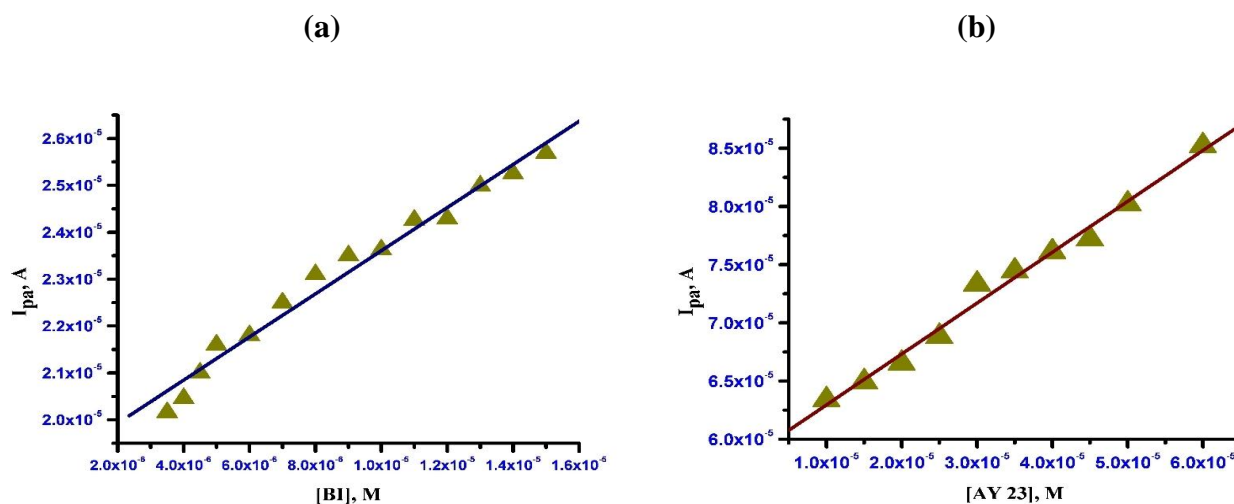


Figure 9. (a) Effect of different concentration BI at TX-100MGPE in 0.1 M PBS at the scan rate of 0.1 V/s, (b) Effect of different concentrations AY 23 at TX-100MGPE in 0.1 M PBS at the scan rate of 0.1 V/s.

The electrochemical response of peak current of AY 23 was increased linearly with the concentration. The limit of detection was calculated using the following formula, $LOD = 3S/N$, where S is the standard deviation of blank and N is the slope of the calibration curve [29-32]. Limit of detection and limit of quantification are used to describe the smallest concentration of an analyte that can be reliably measured by an analytical procedure. The response of peak current of AY 23 at MCPE was linear with the concentration of AY 23 in the range from 1×10^{-5} to 6×10^{-5} M. The detection limit which is obtained for the BI and AY 23 were $0.24 \mu\text{M}$ and $0.25 \mu\text{M}$. The detection limit obtained for the present work is compared with the other report and were tabulated in table.1 and table.2

Table 1. Comparison of the developed electrode with other electrodes for the determination of BI

Electrode	Method	Linear range (M)	Detection limit (M)	Reference
PGMCPE	CV	$2 \times 10^{-6} - 6 \times 10^{-5}$	11×10^{-8}	33
NBE/CPE	DPV	$1 \times 10^{-6} - 1 \times 10^{-4}$	36×10^{-8}	34
SPE	CV	$5 \times 10^{-7} - 1 \times 10^{-4}$	20×10^{-8}	35
SPCE	CV	$5 \times 10^{-7} - 1 \times 10^{-4}$	19×10^{-8}	36
TX-100MGPE	CV	$3.5 \times 10^{-6} - 1.5 \times 10^{-5}$	2.4×10^{-7}	Present work

PGMCPE: Polyglycine modified carbon paste electrode, (NBE/CPE): 4-(4-nitrophenylazo) N- benzyl, N-ethylaniline carbon paste electrode, SPCE: Screen printed carbon electrode, SPE: Screen printed electrode.

Table 2. Comparison of the developed electrode with other electrodes for the determination of AY 23

Electrode	method	Detection limit (M)	Reference
Carbon nanotubes/GCE	DPV	1.88×10^{-7}	37
Acetylene black/GCE	DPV	1.87×10^{-7}	38
SPCE	AdSV	7×10^{-8}	39
PGMCPE	CV	2.83×10^{-7}	40
TX-100MGPE	CV	2.5×10^{-7}	Present work

GCE; Glassy carbon electrode, PGMCPE: Polyglycine modified carbon paste electrode, SPCE: Screen printed carbon electrode

3.8. Repeatability, Reproducibility, and Stability

The reproducibility test of the developed electrode was performed by 3 similar electrodes and cyclic voltammogram was recorded under the similar condition and it was noticed that the relative standard deviation of 2.9 % for 3 measurements shows that the developed electrode has good reproducibility. The repeatability was also evaluated by changing the solution, and observed that the relative standard deviation of 2.6 % for 3 measurements. The stability of the developed electrode was performed by running for CV 44 cycles and the percentage of deviation was calculate which is observed that the percentage of degradation which is less than 1.5% shows that the developed electrode is having good stability.

3.9. Separation of the Voltammetric responses of BI and AY23

The interference of the substance at the modified electrode for the determination of BI and AY 23 was studied under optimum condition. Figure 10a, Shows the CVs and Figure 10b, shows the DPVs of the mixture solution contains AY 23 (1×10^{-4} M) and BI (1.5×10^{-5} M) at TX-100MGPE in 0.1 M PBS (7.5 pH). A well defined two well-separated oxidation peaks were obtained which is corresponding to electrochemical oxidation of BI and AY 23 were obtained.

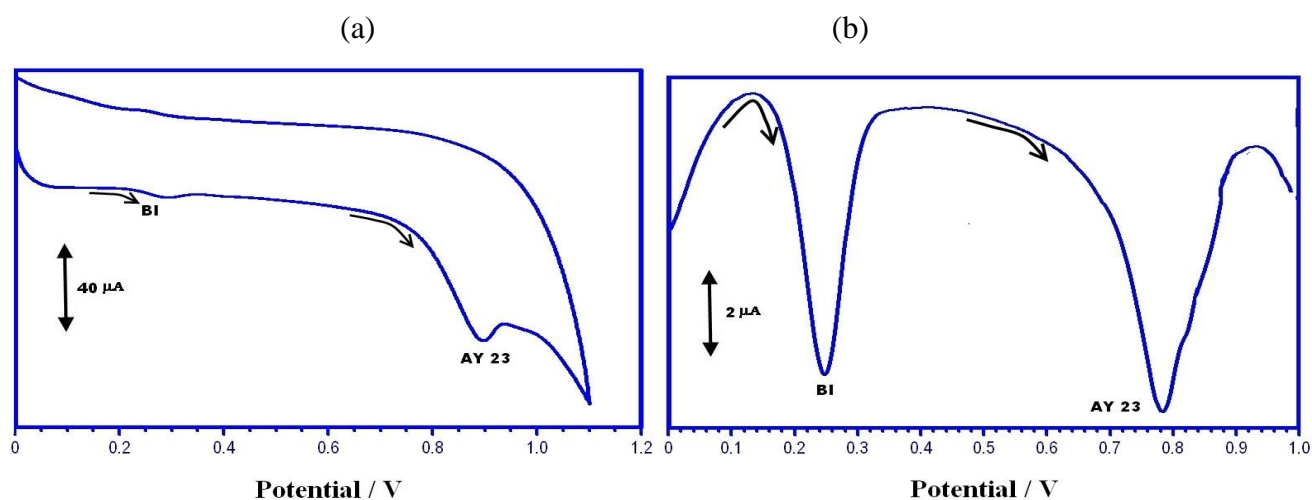


Figure 10. (a) Cyclic voltammogram of AY 23 (1×10^{-4} M) and BI (1.5×10^{-5} M) at TX-100MGPE in 0.1 M PBS (7.5 pH) at the scan rate of 0.1 V/s, (b) Differential pulse voltammogram of AY 23 (1×10^{-4} M) and BI (1.5×10^{-5} M) at TX-100MGPE in 0.1 M PBS (7.5 pH) at the scan rate of 0.1 V/s.

Further different concentration of the one compound keeping constant and keeping other same also studied. Figure.11a shows the CVs of the compounds containing BI (1.5×10^{-5} M) and various concentration of AY 23 (1×10^{-4} - 1.5×10^{-4} M). It was noticed that the peak current of AY 23 increased with the increase of concentration (Figure 11b), when the BI concentration kept constant. In addition, BI peak current and peak potential do not have a significant influence on the AY 23.

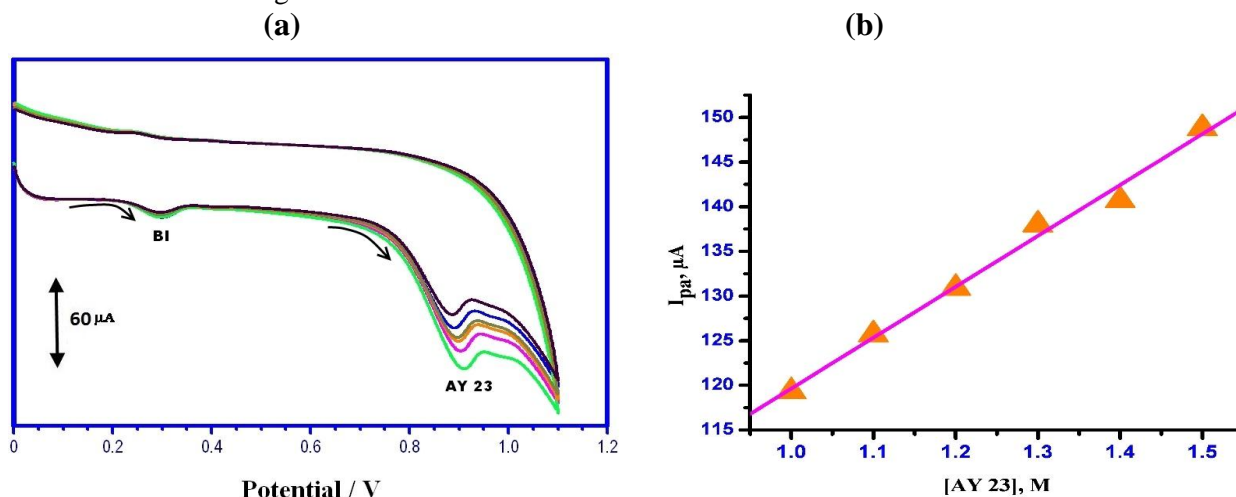


Figure 11. (a) cyclic voltammogram of BI (1.5×10^{-5} M) and various concentration of AY 23 (1×10^{-4} to 1.5×10^{-4} M) in 0.1 M PBS (pH 7.5), (b) various concentration of AY 23 (1×10^{-4} - 1.5×10^{-4} M) Vs. I_{pa}

3.10. Analytical applications

3.10.1. Water sample

Determination of BI and AY 23 in tap water and the laboratory wastewater was performed in order to study the application of developed electrode. Various concentrations of BI and AY 23 were added 5 ml of a water sample, and the experiments were carried out with the help of a supporting electrolyte. It was observed that the recovery was in the range of 100.21% to 106.0% for BI and 100.3% to 100.9% for AY 23.

3.10.2. Food Stuffs

In order to study the applicability of developed electrode for the determination of BI and AY 23 in the food sample, candy-coated chocolate, and soft drink were selected and was purchased from the local market. The recoveries were studied by using the standard addition method. The recovery ranges from 90.2% to 96.6% for BI and 91.5% to 99.3% for AY 23. Recovery ranges show that the developed electrode is very sensitive and a great application for the determination of trace amount of the compounds.

Conclusion

We successfully developed surfactant modified graphene electrochemical sensor, which exhibits a good electrocatalytic response for the oxidation of BI and AY 23 compared to the BGPE associate with the large peak current enhancement. Bare and modified electrodes were characterized by FESEM. Under optimized conditions, the current response was proportional to the concentration in the range 3.5×10^{-6} - 1.5×10^{-5} M for BI and 1×10^{-5} - 6×10^{-5} M for AY 23 with the limit of detection 0.24 μ M and 0.25 μ M. Moreover, the fabricated electrochemical sensor shows simple preparation, good stability, sensitivity, saving time and low cost make the developed method suitable for the determination of BI and AY 23 in the real sample with a satisfactory result.

Acknowledgment-We gratefully acknowledge the financial support from the VGST, Bangalore under Research Project No. KSTePS/VGST (L1) 2016-17/GRD-559/2017-18/126/333.

References

1. P. Ashkenazi, C. Yarnitzky, M. Cais. Determination of synthetic food colours by means of a novel sample preparation system, *Anal Chim Acta*. 248 (1991) 289.
2. S.L.M. Silva, Q.B.S. Garcia, C.F.L.J. Lima, E. Barrado, Voltammetric determination of food colorants using a polyallylamine modified tubular electrode in a multicommutated flow system, *Talanta*. 72 (2007) 282.
3. K. S. Rowe, K. J. Rowe, Synthetic food coloring and behavior: a dose response effect in a double-blind, placebo-controlled, repeated measures study, *J. Pediatr*. 125 (1994) 691.
4. P. L. Lopez de Alba, L. Lopez Martinez, V. Cerda, L. M. De Leon Rodriguez. Simultaneous determination of tartrazine, sunset yellow and allura red in commercial soft drinks by multivariate spectral analysis, *Quim Anal*. 20 (2001) 63.
5. R. Nishimoto, Q. Zhu, T. Miyamoto, T. Sato, X. Tu, Monopersulfate oxidation of acid Orange 7 with an iron(III)-tetrakis(N-methylpyridinium-4-yl)porphyrin intercalated into the layers of montmorillonite and pillared clay, *J Mol Catal A Chem*. 396 (2015) 84.
6. G. Zhang, I. Okajima, T. Sako, Decomposition and decoloration of dyeing wastewater by hydrothermal oxidation, *J. Supercrit Fluids*. 112 (2016) 136.
7. M. Khayet, A. Y. Zahrim, N. Hilal, Modelling and optimization of coagulation of highly concentrated industrial grade leather dye by response surface methodology, *Chem Eng J*. 167 (2011) 77.
8. S. Brosillon, H. Djelal, N. Merienne, A. Amrane,) Innovative integrated process for the treatment of azo dyes: coupling of photocatalysis and biological treatment, *Desalination*. 222 (2008) 331.
9. M. A. Oturan, J. J. Aaron, Advanced oxidation processes in water/wastewater treatment: principles and applications. A review, *Crit Rev Environ Sci Technol*. 44 (2014) 2577.
10. M. Panizza, G. Cerisola, Application of diamond electrodes to electrochemical processes, *Electrochim Acta*. 51, (2005) 191.
11. M. Panizza, G. Cerisola, Direct and mediated anodic oxidation of organic pollutants, *Chem Rev*. 109 (2009) 6541.
12. N. P. Shetti, S. J. Malode, R. S. Malladi, S. L. Nargund, S. S. Shukla, T. M. Aminabhavi, Electrochemical detection and degradation of textile dye Congo red at graphene oxide modified electrode, *Microchem. J*. 146 (2019) 387.
13. N. P. Shetti, D. S. Nayak, S. J. Malode, Electrochemical behavior of azo food dye at nanoclay modified carbon electrode-a nanomolar determination, *Vacuum*. 155 (2018) 524.
14. N. P. Shetti, D. S. Nayak, G. T. Kuchinad, Electrochemical oxidation of erythrosine at TiO₂ nanoparticles modified gold electrode—An environmental application, *J. Environ. Chem. Eng*. 5 (2017) 2083.
15. C.H. Lu, H.H. Yang, C.L. Zhu, X. Chen, G.N. Chen, A graphene platform for sensing biomolecules, *Angew. Chem. Int. Ed*. 48 (2009) 4785.
16. M. Zhou, Y.M. Zhai, S.J. Dong, Electrochemical sensing and biosensing platform based on chemically reduced graphene oxide, *Anal. Chem*. 81 (2009) 5603.

17. Y. Wang, Y.M. Li, L.H. Tang, J. Lu, J.H. Li, Application of graphene-modified electrode for selective detection of dopamine, *Electrochem. Commun.* 11 (2009) 889.
18. S. Alwarappan, A. Erdem, C. Liu, C.Z. Li, Probing the Electrochemical Properties of Graphene Nanosheets for Biosensing Applications, *J. Phys. Chem. C.* 113 (2009) 8853.
19. N.G. Shang, P. Papakonstantinou, M. McMullan, M. Chu, A. Stamboulis, Catalyst-Free Efficient Growth, Orientation and Biosensing Properties of Multilayer Graphene Nanoflake Films with Sharp Edge Planes, *Adv. Funct. Mater.* 18 (2008) 3506.
20. L.Tang, Y. Wang, Y. Li, H. Feng, J. Lu, J. Li, Preparation, Structure, and Electrochemical Properties of Reduced Graphene Sheet Films, *Adv. Funct. Mater.* 19 (2009) 2782.
21. N. P Shetti, D. S Nayak, S. J Malode, R. M. Kulkarni, D. B Kulkarni, R. A Teggi, V. V Joshi, Electrooxidation and determination of flufenamic acid at graphene oxide modified carbon electrode, *Surf. Interfac.* 9 (2017)107.
22. W. Kemula, Z. Kublik, Observation of Transient Intermediates in Redox Processes by Variable Voltage Oscillo-polarography and Cyclic Voltammetry, *Nature.* 182 (1958) 793.
23. S. Reddy, B. E. Kumara Swamy, H.N. Vasan, H. Jayadevappa, ZnO and ZnO/polyglycine modified carbon paste electrode for electrochemical investigation of dopamine, *Anal. Methods.* 4 (2012) 2778.
24. S Chitravathi, S. Reddy, B.E. Kumara Swamy, Electrochemical determination of ezetimibe by MgO nanoflakes-modified carbon paste electrode, *J. Electroanal. Chem.* 764 (2016) 1.
25. C. Raril, J.G. Manjunatha, Carbon Nanotube Paste Electrode for the Determination of Some Neurotransmitters: A Cyclic Voltammetric Study, *Mod. Chem. Appl.* (2018) 6:3.
26. S. Reddy, B. E. Kumara Swamy, H. Jayadevappa, CuO nanoparticle sensor for the electrochemical determination of dopamine, *Electrochim. Acta.* 61 (2012) 78.
27. S. D. Bukkitgar, N. P. Shetti, Electrochemical behavior of anticancer drug 5-fluorouracil at carbon paste electrode and its analytical application, *J. Anal. Sci. Technol.* 7 (2016)1.
28. E. Laviron, General expression of the linear potential sweep voltammogram in the case of diffusionless electrochemical systems, *J. Electroanal. Chem. Interfacial Electrochem.* 101 (1979) 19.
29. G. Tigari, J. G. Manjunatha, C. Raril, N. Hareesha, Determination of Riboflavin at Carbon Nanotube Paste Electrodes Modified with an Anionic Surfactant, *Chemistry Select.* 4 (2019) 2168.
30. J. G. Manjunatha, M. Deraman, N. H. Basri, N. S. Mohd Nor, I.A. Talib, N. Ataollahi, Sodium dodecyl sulfate modified carbon nanotubes paste electrode as a novel sensor for the simultaneous determination of dopamine, ascorbic acid, and uric acid, *C. R. Chim.* 17 (2014) 465.
31. A. M. Bagoji, S. T. Nandibewoor, Redox behavior of riboflavin and its determination in real samples at graphene modified glassy carbon electrode, *Phys.chem.Commun.* 3 (2016) 65.
32. N. P. Shetti, D. S. Nayak, Electrochemical detection of chlorpheniramine maleate in the presence of an anionic surfactant and its analytical applications, *Can. J. Chem.* 95 (2017) 553.
33. J. G Manjunatha, A novel poly (glycine) biosensor towards the detection of indigo carmine: A voltammetric study, *J. food. Drug. Anal.* 26 (2018) 292.
34. A. Majid, S. Mehrnoosh, S. A. Masoomah, M. Asadollah, Mediated electrochemical method for the determination of indigo carmine levels in food products, *Talanta.* 173 (2017) 60.
35. M. Diaz-Gonzalez, C. Fernandez-Sanchez, C. Garcia, Comparative Voltammetric Behavior of Indigo Carmine at Screen-Printed Carbon Electrodes, *Electroanal.* 14 (2002) 665.
36. T. A. Silva, G. F. Pereira, O. Fatibello-Filho, K. I. B. Eguiluz, G. R. Salazar-Banda, Electroanalytical sensing of indigo carmine dye in water samples using a cathodically pretreated boron-doped diamond electrode, *J. Electroanal. Chem.* 769 (2016) 28.
37. Y. Xiaofeng, Q. Haibin, G. Miaomiao, Z. Huajie, Simultaneous detection of Ponceat 4R and tartrazine in food using adsorptive stripping voltammetry on an acetylene black nanoparticle-modified electrode, *J. Sci. Food Agri.* 91 (2001) 2821.
38. Z. Wang, Y. Shan, L. Xu, G. Wu, X. Lu. Development and application of the tartrazine voltammetric sensors based on molecularly imprinted polymers, *Int. J. Polym. Anal. Charact.* 22 (2016) 83.
39. Y. Perdomo, V. Arancibia, O. Garcia-Beltran, E. Nagles. Adsorptive Stripping Voltammetric Determination of Amaranth and Tartrazine in Drinks and Gelatins Using a Screen-Printed Carbon Electrode. *Sensors.* 17 (2017) 1.
40. J. G. Manjunatha, A novel voltammetric method for the enhanced detection of the food additive tartrazine using an electrochemical sensor. *Heliyon.* (2018) 4.

(2019) ; <http://www.jmaterenvironsci.com/>